Testing a glacial erosion rule using hang heights of hanging valleys, Jasper National Park, Alberta, Canada

J. M. Amundson[1] and N. R. Iverson[2]

Received 24 June 2005; revised 29 November 2005; accepted 20 December 2005; published 18 March 2006.

[1] In most models of glacial erosion, glacier sliding velocity is hypothesized to control rates of bedrock erosion. If this hypothesis is correct, then the elevation difference between hanging and trunk valley floors, the hang height, should be dictated by the relative sliding velocities of the glaciers that occupied these valleys. By considering sliding velocity to be proportional to balance velocity and using mass continuity, hang height is expressed in terms of glacier catchment areas, slopes, and widths, which can be estimated for past glaciers from the morphology of glacial valleys. These parameters were estimated for 46 hanging valleys and their trunk valleys in three adjacent regions of Jasper National Park. The variability in valley morphology can account for 55–85% of the hang height variability if erosion rate scales with balance velocity raised to a power of 1/3. This correspondence is in spite of spatial variations in glaciation duration, snow accumulation rates, and other variables that likely affected hang heights but cannot be readily estimated and so are not included in our formulation. Thus it appears that balance velocity, and by extension, sliding velocity if the two are proportional, may be a reasonable control variable for assessing erosion rate.

Citation: Amundson, J. M., and N. R. Iverson (2006), Testing a glacial erosion rule using hang heights of hanging valleys, Jasper National Park, Alberta, Canada, *J. Geophys. Res.*, *111*, F01020, doi:10.1029/2005JF000359.

1. Introduction

[2] During the last decade, interest in glacial erosion has intensified due to its likely effect on uplift in orogenic belts, weathering rates, and atmospheric CO_2 [*Hallet et al.*, 1996; *Jaeger et al.*, 2001]. Addressing these problems and longstanding problems of glacial landscape evolution requires erosion models that can be applied over large areas (e.g., orogens) for long periods (10^5–10^6 yr). Obstacles to testing such models include poorly known initial conditions and mass balance inputs and geological heterogeneity that is difficult to characterize. Nevertheless, several illustrative numerical models have been constructed [*Oerlemans*, 1984; *Harbor*, 1992; *Braun et al.*, 1999; *MacGregor et al.*, 2000], and some characteristic landforms have been generated, including U-shaped valleys and overdeepenings in longitudinal valley profiles. Recent additional insights have been provided by an analytical model for the development of longitudinal valley profiles [*Anderson et al.*, 2006].

[3] Central to these models is an erosion rule that relates erosion rate to glaciological variables. In most models, erosion rate is assumed to be a function of sliding velocity [e.g., *Oerlemans*, 1984; *Harbor*, 1992; *Braun et al.*, 1999; *MacGregor et al.*, 2000] or ice discharge [*Anderson et al.*, 2006]; measurements of surface velocity and sediment discharge from Bench Glacier, Alaska, support this assumption [*Riihimaki et al.*, 2005]. This also agrees with the leading model of glacial abrasion [*Hallet*, 1979], in which sliding velocity governs both the flux of abrasive particles across the bed and particle-bed contact forces. Whether rates of quarrying, the process by which ice fractures the bed and dislodges rock fragments, also depend primarily on sliding velocity is less clear. Mechanical models assume that quarrying rates are limited by rates of crack growth in the bed, which are thought to be accelerated by water-filled cavities down glacier from bedrock bumps [*Iverson*, 1991; *Hallet*, 1996]. As these cavities grow, normal stresses where ice contacts the bed increase, promoting crack growth. Cavity size depends on sliding velocity but also on effective pressure: the difference between the ice overburden pressure and water pressure in cavities [*Walder*, 1986; *Hallet*, 1996]. Besides affecting cavity size, cavity water pressure also controls the fluid pressure within cracks in the rock, potentially influencing crack growth rates [*Iverson*, 1991]. Also, water pressure fluctuations are likely to be important because they maximize both ice-rock stresses and pore pressure gradients within bedrock [*Iverson*, 1991; *Hallet*, 1996].

[4] Given the mechanical complexity of quarrying, as well as arguments and observations that it is volumetrically

[1]Geophysical Institute, University of Alaska Fairbanks, Fairbanks, Alaska, USA.
[2]Department of Geological and Atmospheric Sciences, Iowa State University, Ames, Iowa, USA.

0148-0227/06/2005JF000359$09.00

more important than abrasion [*Jahns*, 1943; *Boulton*, 1979; *Drewry*, 1986; *Iverson*, 2002; *Loso et al.*, 2004], can simple velocity-based erosion rules adequately characterize erosion rates and generate glacial landscapes? Using a numerical model that incorporated a velocity-based erosion rule, *MacGregor et al.* [2000] were able to produce hanging valleys, which form because tributary glaciers erode rock more slowly than trunk glaciers. In their study, hang height, the difference in elevation between the floors of hanging and trunk valleys, depended on the relative discharges of tributary and trunk glaciers and increased with distance down the trunk valley for hanging glaciers with similar ice fluxes. We make a similar assumption: that erosion rate depends on balance velocity, and by extension, sliding velocity. However, rather than modeling the erosion of glacial valleys on that basis, we test the assumption empirically by studying hanging valleys in Jasper National Park, Alberta. By using valley morphology as an indicator of balance velocity and assuming that sliding velocity is proportional to balance velocity, we test whether observed hang heights can be explained by an erosion rule in which long-term erosion rates depend on sliding velocity.

2. Rationale

[5] We seek an empirical means of testing whether an erosion rule based only on sliding velocity is applicable over the long periods required for erosion of valleys. Using a velocity-based erosion rule, together with mass continuity and the approximation for the basal shear stress of a valley glacier, a relationship is obtained for the hang height in terms of the plan view areas, widths, and slopes of a tributary glacier and adjacent trunk glacier. The relationship is tested by estimating these parameters from the morphologies of hanging and trunk valleys as determined from topographic maps.

[6] Our formulation, by necessity, neglects the spatial variability of a number of factors that likely affect the variability of hang heights, but are poorly known during glaciation. The most important of these factors follow.

[7] 1. Glaciers wax and wane during valley erosion; the timing and duration of glaciation varies among valleys in a given region. Although most erosion may occur during glacial maximums, the chronology of glacier occupation in a particular region is seldom known well enough to constrain this issue, particularly since valley erosion usually extends over more than one glacial cycle.

[8] 2. Proportions of basal motion and internal ice deformation vary among glaciers and depend on a number of factors, including bed type, water discharge at the bed and associated effective pressure, and ice temperature. For modern wet-based valley glaciers, ratios of basal motion to surface velocity are highly variable, ranging from 0.1 to 0.9 [*Paterson*, 1994, p. 135], although within a particular region there is typically less variability.

[9] 3. Erosion due to nonglacial processes, such as fluvial incision and mass wasting, varies spatially and occurs during periods when all or part of the landscape is ice free.

[10] 4. Dynamic coupling at the confluences of tributary and trunk glaciers gives rise to longitudinal stress gradients, which differ from one confluence to another.

[11] 5. Snow accumulation rates vary in a given region and can differ considerably between adjacent catchments.

[12] 6. Resistance to erosion depends on bedrock lithology and structure. These can be estimated from maps, but a meaningful way to quantify resistance to erosion that considers rock strength and hardness, joint orientation and density, and other properties is unclear.

[13] 7. Basal shear stresses vary among glaciers, although the nonlinearity of the flow law of ice suppresses that variability; for glaciers on hard beds, basal shear stresses typically range from 50–150 kPa [*Paterson*, 1994, p. 242].

[14] These factors may strongly influence hang height variability. Our neglect of the variability of any one of them does not constitute an assumption or approximation but an acknowledgment that its variability during glacial cycles cannot readily be estimated. By neglecting these factors in the following formulation, we test the hypothesis that the effect of their variability on hang heights is small compared to the effects of glacier areas, widths, and slopes. These latter variables can be estimated from maps and may be first-order controls on ice flux, balance velocity, and sliding velocity. Thus this hypothesis is worth pursuing, despite the necessity of neglecting the variability of some factors that cannot be estimated.

3. Formulation

[15] If sliding velocity dictates erosion rate, the hang height of a hanging valley will reflect the difference in sliding velocity between a trunk and tributary glacier. Consider an erosion rule of the form

$$\dot{e} = CU_s^n, \tag{1}$$

where $\dot{e}$ is the erosion rate (thickness of rock eroded per unit time), C is a constant that depends inversely on the erosion resistance of bedrock, U_s is the basal sliding velocity, and n is a constant. The erosion rule presented in equation (1) is intended to express long-term erosion rates; in this study, U_s indicates the temporally averaged sliding velocity at the glacier centerline. Integer values of n ranging from 1 to 4 are often assumed in models [e.g., *Harbor*, 1992; *MacGregor et al.*, 2000]. Following the nomenclature of *MacGregor et al.* [2000], the hang height, H, is defined as the elevation difference between hanging and trunk valley floors. If hanging and trunk valleys have the same values of C and have been eroded for the same duration, T, then from equation (1)

$$H = CT\left(U_{st}^n - U_{sh}^n\right), \tag{2}$$

where U_{st} and U_{sh} are the sliding speeds near the confluences of glaciers that occupied the trunk and hanging valleys, respectively. With equation (2), we assume that tributary and trunk river valleys that preceded glaciation were graded to each other. Ultimately, we wish to express sliding velocity as a function of glacier geometry. One approach is to let the sliding velocity be some fraction, λ, of the balance velocity, which can be expressed in terms of glacier geometry:

$$U = \frac{A\dot{a}}{hw}, \tag{3}$$

where U is the balance velocity, A is the accumulation area, $\dot{a}$ is the mean accumulation rate of ice over that area, h is the centerline ice thickness, and w is the depth-averaged width. Equation (3) applies to the accumulation zone of a glacier only and assumes that glacier flow is in balance. Substituting equation (3) into equation (2) yields

$$H = CT(\dot{a}\lambda)^n \left[\left(\frac{A_t}{h_t w_t} \right)^n - \left(\frac{A_h}{h_h w_h} \right)^n \right]. \quad (4)$$

Of the variables in equation (4), H, A, and w can be estimated from topographic maps, and we will neglect the variability of C, T, $\dot{a}$, and λ (see section 2). Although ice thickness, h, strongly influences glacier velocity and is highly variable spatially, it is not easily measured from maps (see section 4). A better approach is to use valley morphology to estimate glacier surface slope; estimated slopes can be tested by measuring glacier length and comparing the length-slope relationship to the well-known inverse relationship for modern glaciers [*Clarke*, 1991]. Hang height is affected by glacier slope through its effect on basal shear stress:

$$\tau_b = S\rho g h \sin\alpha, \quad (5)$$

where τ_b is the basal shear stress of a valley glacier at its centerline, S is a shape factor between 0.5 and 1.0 that accounts for the shape of the transverse valley profile, ρ is the ice density, g is gravitational acceleration, and α is the glacier surface slope [*Paterson*, 1994, p. 268]. Rearranging equation (5) and inserting it into equation (4) gives

$$H = C_1 \Psi, \quad (6)$$

where

$$C_1 = CT \left(\frac{S\rho g \dot{a} \lambda}{\tau_b} \right)^n \quad (7)$$

and

$$\Psi = \left(\frac{A_t \sin\alpha_t}{w_t} \right)^n - \left(\frac{A_h \sin\alpha_h}{w_h} \right)^n. \quad (8)$$

C_1 is not a constant because some of the variables in equation (7) will differ among glaciers. Without a means of estimating that variability for past glaciers, however, we treat C_1 as a constant and thereby test the hypothesis that its variability is small relative to the variability of Ψ.

[16] We now have a relationship between hang height and valley morphology that can be tested with measurements from topographic maps. If the form of the erosion rule (equation (1)) is correct and the variability of C_1 is small relative to that of Ψ for tributary and trunk glaciers of a particular region, then H and Ψ will be linearly correlated. Moreover, if areas, slopes, and widths of glaciers are known, n can be constrained by adjusting its value to optimize the closeness of the correlation between H and Ψ.

[17] By treating balance velocity as a proxy for sliding velocity, we are exploring the relationship between erosion rate and ice flux. One motivation for this approach is that balance velocity is relatively easy to compute, making it a favorable input parameter for an erosion model. An alternative approach is to substitute a sliding rule into equation (2). Although that would introduce a minimum of two more parameters with unknown variability, it yields a relationship very similar in form to equations (6)–(8) (see Appendix A).

[18] Ideally, equation (8) would be applied precisely at confluences, where hangs develop. However, longitudinal stress gradients arising there due to trunk-tributary interaction would violate the simple relation for basal shear stress in our formulation (equation (5)) [*Paterson*, 1994, p. 268]. Because of the neglect of these stress gradients, equation (8) applies to regions sufficiently far upstream from confluences to be outside the zone of dynamic trunk-tributary interaction. We thus adopt the viewpoint that hang height reflects primarily the independent dynamics of a trunk glacier and its tributary, rather than their dynamic interaction at the confluence. This approximation is necessary because longitudinal stress gradients cannot be readily estimated at the confluences of past glaciers.

[19] An important ramification of this approximation is that it ensures the formulation for Ψ is not circularly biased toward correlation with hang height. Ψ depends on the quantity $\left(\frac{A_t}{h_t w_t} \right)^n - \left(\frac{A_h}{h_h w_h} \right)^n$ (see equation (4)), and thus tends to be proportional to the difference in thickness between trunk and tributary glaciers, $h_t - h_h$. The observation that the surfaces of tributary glaciers are commonly graded to the surfaces of trunk glaciers implies that $h_t - h_h$ equals the hang height, which would appear to bias correlations of hang height with Ψ. However, the grading of the surfaces of tributaries with their trunk glaciers reflects their dynamic interaction at confluences and the associated development of longitudinal stress gradients; without these local stress gradients, $h_t - h_h$ would not equal hang height. Thus, because Ψ is formulated to depend on the independent fluxes of ice emerging from trunk and tributary catchments, there is no requirement that $h_t - h_h$ equals hang height and hence no circularity in the formulation of Ψ.

4. Settings and Methods

[20] This study focused on hanging valleys feeding the Athabasca and Sunwapta River valleys in southern Jasper National Park, Alberta, Canada (Figure 1). The valleys now occupied by these rivers were widened and deepened through multiple glacier advances. During periods of the Wisconsin glaciation, ice inundated this part of the Canadian Rockies and coalesced with the Laurentide ice sheet on the plains to the northeast [*Yorath and Gadd*, 1995]. Some erosion also likely occurred during previous glaciations. The strong U-shaped geometry of most valleys in this region suggests that during the recent past fluvial incision and mass wasting were minor processes of erosion compared to glacial erosion. Furthermore, reconstructions of the Cordilleran and Laurentide ice sheets [e.g., *Hughes*, 1998, chap. 9] suggest that glaciers that occupied valleys in this region (at an elevation of 1000–3000 m) may have been entirely in the accumulation zone for much of the Wisconsin glaciation, which is consistent with the application of equation (3).

[21] We studied hanging valleys associated with three major trunk-valley segments: the Sunwapta River

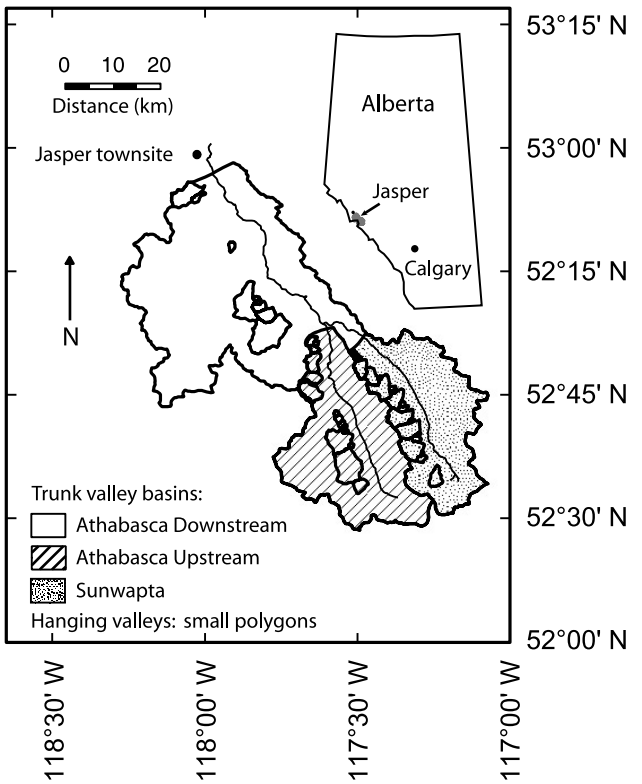

Figure 1. Study area in western Alberta, Canada. Catchments of hanging valleys are represented by small polygons within the three trunk valley basins.

(Sunwapta), the Athabasca River upstream from its confluence with the Sunwapta River (Athabasca upstream), and the Athabasca River between this confluence and the town of Jasper (Athabasca downstream) (Figure 1). 46 hanging valleys were considered. Of these, 22 feed the Sunwapta segment, 15 feed the Athabasca upstream segment, and 9 feed the Athabasca downstream segment.

[22] Although the bedrock lithology in this area is highly variable, the geologic setting is relatively well suited for this study. Trunk valleys lie approximately parallel to the strikes of thrust faults. Tilted Precambrian and early Paleozoic strata (dominantly carbonates, quartzite, shale, and slate) strike roughly parallel to these faults [*Yorath and Gadd*, 1995], minimizing lithologic variability along the lengths of the trunk-valley segments. For the same reason, hanging valleys generally cut across the strike of rock strata. Thus, although a given hanging valley is cut into multiple rock units with different resistances to erosion, hanging valleys feeding one side of a trunk valley tend to cut through similar sequences of rock strata. Of course, trunk valleys may be eroded in strata with overall resistances to erosion that are different from the strata of hanging valleys. However, given that trunk valleys lie parallel to the strike of strata, differences in erosion resistance between hanging valleys and the trunk valley of a given catchment will tend to be uniform and thus not affect the strength of correlations between hang height and Ψ.

[23] Hanging valleys feeding only the southwestern sides of trunk-valley segments were studied (Figure 1). Because strata tend to dip moderately to the southwest, the southwestern slopes of trunk valleys are generally steeper, with more pronounced hanging valleys than northeastern slopes.

[24] Our hypothesis, as expressed by equations (6)–(8), is that if balance velocity controlled erosion rate and the spatial variability of C_1 was not too large, then hang heights should be related to the areas, slopes and widths of tributary and trunk glaciers, as given by (equation (8)). These variables were estimated using GIS software to make measurements from ten 1:50,000 digital topographic maps [*Natural Resources Canada*, 1994a, 1994b, 1994c, 1994d, 1994e, 1994f, 1994g, 1994h, 1994i, 1994j].

[25] To determine hang heights of hanging valleys, the top and bottom of hangs were defined. Hang tops were taken as the elevation of the point of maximum convexity in the longitudinal profile of the hanging valley near its mouth. Hang bases were taken as the elevation where the stream from the hanging valley joined that of the trunk valley. If no stream drained the hanging valley, the mean azimuth of the axis of the hanging valley was extrapolated to where it intersected the trunk-valley river, and the elevation of that point was used. Although alluvium mantles valley floors in some areas, its thickness is usually poorly known, so hang heights were not adjusted to account for this alluvium.

[26] Glacier areas upstream from confluences were estimated by measuring catchment areas defined by topographic divides. Because of steep valley walls, catchment areas reasonably approximate areas of former glaciers. There was uncertainty demarcating some valley mouths, but uncertainties were small relative to total catchment areas.

[27] We chose to approximate glacier slope by measuring the mean slope of the valley floor because trimlines, moraines, and other geomorphic features commonly used to infer slope reflect recent, discrete glacial episodes rather than the much longer period over which hanging valleys likely formed. Our elevation and length measurements needed to calculate mean bed slope extended from the lowest point on drainage divides (saddles) to valley mouths. This method probably overestimated glacier slope but provided an internally consistent approximation. An inverse relationship between lengths and slopes of modern glaciers [e.g., *Clarke*, 1991], determined from the World Glacier Inventory data set [*National Snow and Ice Data Center*, 2003], predicted slopes similar to those inferred from our measurements, with a root mean square error of 1.9° (see Figure 2). The length-slope relationship is particularly strong for long glaciers; the observation that our surface slope estimates closely match the regression from the World Glacier Inventory data set (Figure 2b) provides support for our slope estimates.

[28] The depth-averaged widths of former tributary and trunk glaciers were estimated just up glacier from their former confluences. Surface width was estimated by using the point of maximum convexity at the edges of transverse valley profiles to approximate the former position of lateral margins. Depth-averaged width is proportional to surface width; for example, for the common case of a parabolic profile [e.g., *Harbor and Wheeler*, 1992] depth-averaged width is two thirds the surface width. By incorporating the constant of proportionality into C_1, we use the surface width in our calculations. Although actual time-averaged glacier widths likely deviated from estimated values, our rough estimation procedure is preferable to treating width as a constant.

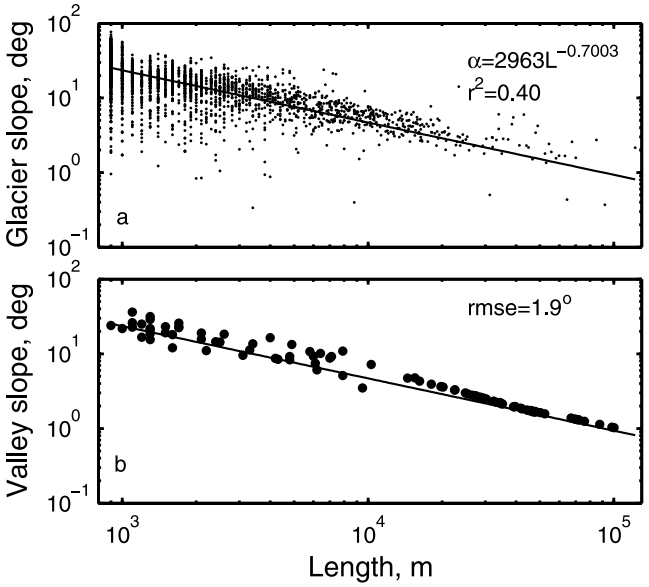

Figure 2. (a) Power law relationship between glacier slope, α, and length, L, is determined from the World Glacier Inventory North American data set [after *Clarke*, 1991]. (b) Regression line in Figure 2a superimposed on data from this study.

[29] Glacier thickness, which we have eliminated from our formulation in favor of using glacier slope, is more difficult to estimate from maps than surface width, and unlike estimates of slope, thickness estimates cannot be tested with data from modern glaciers. The point of maximum valley wall convexity could be used to estimate the elevation of the ice surface near confluences, but owing to steep valley walls, estimates of elevation are more sensitive to errors in assigning the point of maximum convexity than are estimates of ice margin position. More importantly, there is no empirical relationship between glacier thickness and length for modern glaciers that can be used to evaluate the accuracy of thickness estimates. In contrast, the length-slope relationship for modern glaciers [*Clarke*, 1991] provides independent support for our estimates of slope (Figure 2).

5. Results

[30] Our estimation of the areas, slopes, and widths of former glaciers allow hang height to be correlated with Ψ (equation (6)). The value of the sliding velocity exponent in the erosion rule, n (equation (1)), is needed to calculate Ψ but is poorly known. We therefore searched for the value of n that optimized the coefficient of determination (r^2) for a linear least squares regression of H on Ψ (Figure 3). The maximum coefficient of determination (r^2_{max} = 0.60) was found when $n \approx 1/3$.

[31] In Figure 4, hang height is plotted as a function of Ψ using n = 1/3. Figure 4a illustrates this relationship for all

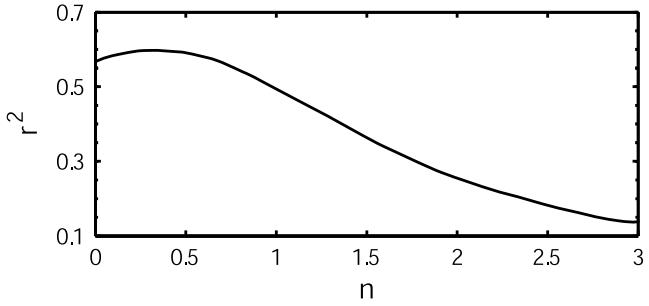

Figure 3. Coefficients of determination (r^2) for n ranging from 10^{-4} to 3. r_{max}^2 = 0.60 at n = 1/3.

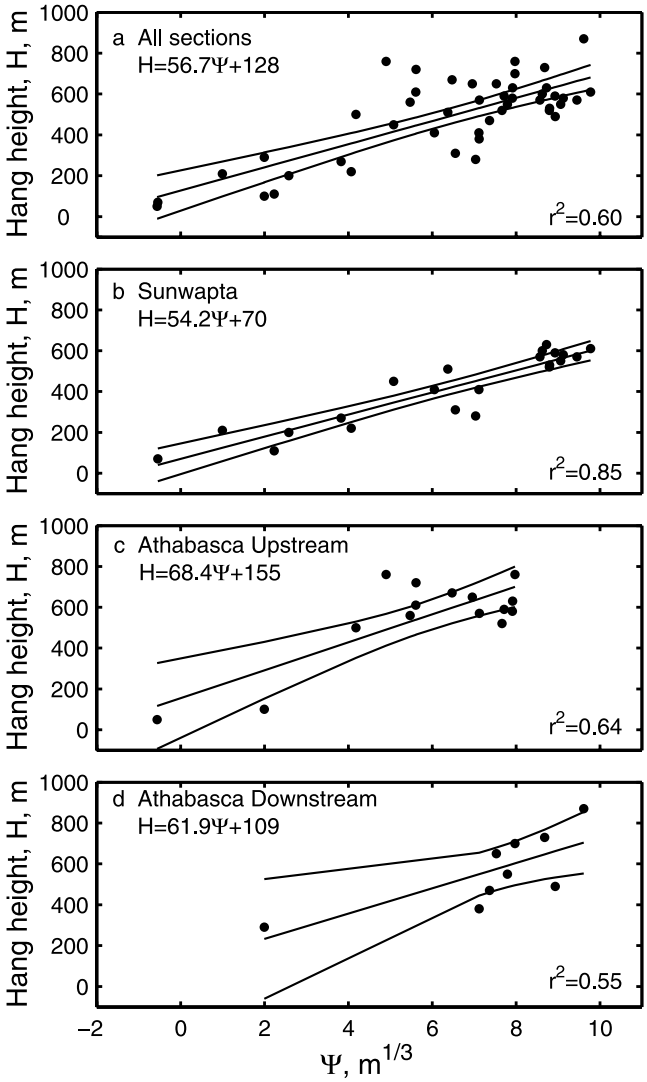

Figure 4. Hang height as a function of Ψ with n = 1/3 for all hanging valleys (Figure 4a) and for those of each region (Figures 4b–4d). (a) Standard errors of the slope of the regression line and of the hang height at Ψ = 0 are 7.0 $m^{1/3}$ and 49 m, respectively. The F statistic is 65.0; the probability of no association between hang height and is less than 0.0001 [*Snedecor and Cochran*, 1980, p. 181]. (b) Standard errors are 5.1 $m^{1/3}$ and 36 m. The F statistic is 112.7; the probability of no association is less than 0.0001. (c) Standard errors are 14.4 $m^{1/3}$ and 90 m. The F statistic is 22.7; the probability of no association is 0.0004. (d) Standard errors are 21.2 $m^{1/3}$ and 164 m. The F statistic is 8.5; the probability of no association is 0.0225. The curved lines indicate 95% confidence intervals of the regressions.

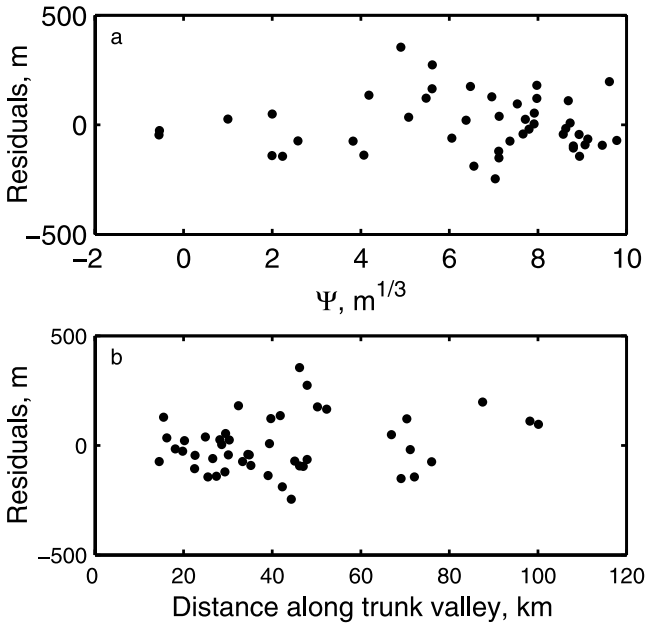

Figure 5. Residuals determined from a linear least squares regression of H on Ψ, as a function of (a) Ψ and (b) distance down the trunk valley.

hanging valleys in the study area. 60% of the variance in hang height ($r^2 = 0.60$) can be attributed to its regression on Ψ [*Snedecor and Cochran*, 1980, p. 181]. Furthermore, plots of the residuals indicate that there is no systematic variability in C_1 nor systematic measurement error as a function of either Ψ or distance down the trunk valley (Figure 5). The linear regression does not satisfy the criterion that as Ψ approaches zero, the hang height approaches zero: at $\Psi = 0$ the regression yields a hang height of 128 m ± 49 m. However, the correlation does not weaken significantly when the regression is forced through the origin ($r^2 = 0.53$).

[32] Figures 4b–4d show hang height as a function of Ψ for each of the three regions. The variable Ψ can account for most of the variance of hang height in the Sunwapta region ($r^2 = 0.85$) (Figure 4b), with somewhat weaker correlations in the two Athabasca regions ($r^2 = 0.64$, $r^2 = 0.55$) (Figures 4c and 4d). The slopes of the regression lines, which equal C_1 (equation (6)), differ by less than 26%.

[33] Our formulation for Ψ (equation (8)) can be further evaluated by systematically incorporating various combinations of the variables A, α, and w, into the constant C_1 and comparing the resultant values of Ψ with hang height. Values of r^2 are consistently reduced if the measured variability of one or more of these variables is omitted from the formulation of Ψ (Table 1), indicating that each parameter is important in our analysis.

6. Discussion

[34] Hang height, and therefore erosion rate, is correlated with Ψ, which is derived from the difference in balance velocity between a trunk and tributary glacier. Our results indicate that Ψ accounts for 55–85% of the variability in hang height. The remaining variability can be attributed to spatial variations in bedrock geology, ice accumulation rates, glaciation duration, and other parameters contained in C_1, and to errors in our estimates of glacier area, slope and width. Some of the remaining variability may also reflect too simple an erosion rule. Our results indicate that Ψ accounts for most of the hang height variability with an erosion rule in which balance velocity is raised to a power of 1/3, rather than to a higher integer value commonly assumed in models [e.g., *Harbor*, 1992; *MacGregor et al.*, 2000]. If sliding velocity is proportional to balance velocity, then this exponent agrees with one of the few laboratory studies of sliding and rock erosion by temperate ice [*Budd et al.*, 1979]. However, the significance of this agreement is uncertain; erosional processes in those experiments, which were conducted over periods of hours with bed roughness elements of wavelength less than 10 mm, may have been quite different from those that operate beneath glaciers over much larger time and length scales.

[35] The disparate r^2 values for the three regions (Figures 4b–4d) cannot be adequately explained with the data at hand. Either the errors in estimating glacier area, width, and slope or the variability of C_1 differed among regions. There is no obvious reason why measurement errors would have been higher in some regions than in others. The value of C_1 depends on C, T, S, $\dot{a}$, λ and τ_b and among these variables, only erosion resistance (C) and shape factor (S) can be estimated from maps. The variability of these factors is not obviously different for the three regions. The smaller r^2 values in the two Athabasca regions may, in part, reflect the smaller number of hanging valleys in those regions. The similar slopes of the regressions (Figure 4) indicate that mean values of C_1 were similar for the three regions, despite differences in the apparent variability of C_1.

[36] Our empirical results are consistent with the modeling results of *MacGregor et al.* [2000]. They predicted, as a direct result of erosion rate scaling with sliding velocity, an increase in hang height with distance down the trunk valley for tributary glaciers of similar discharge and an inverse relationship between hang height and the ratio of tributary to trunk glacier discharge. Although we cannot measure ice discharge from maps, we can treat the ratio $\frac{A \sin \alpha}{w}$ as a discharge proxy, $\tilde{Q}$. If we consider the catchment with the most hanging valleys (Sunwapta), calculate the discharge proxy for each hanging valley, $\tilde{Q}_h$, and group the data on that basis, we indeed observe an increase in hang height with distance down the trunk valley (Figure 6a). Furthermore, if hang height is plotted as a function of $\tilde{Q}_h/\tilde{Q}_t$, where $\tilde{Q}_t$ is the discharge proxy for trunk valleys (Figure 6b), there is a clear inverse relationship similar to that of *MacGregor et al.* [2000, Figure 4]. Although neither study conclusively indicates that erosion rate is controlled

Table 1. Highest Coefficients of Determination (r^2) From Least Squares Regression of H_s on Ψ, Using $n = 1/3$ and Moving Additional Parameters From Ψ (Equation (8)) to C_1 (Equation (7))

Parameters included in C_1	r^2
α	0.46
w	0.52
A	0.22
α, w	0.32
α, A	0.26
w, A	0.25

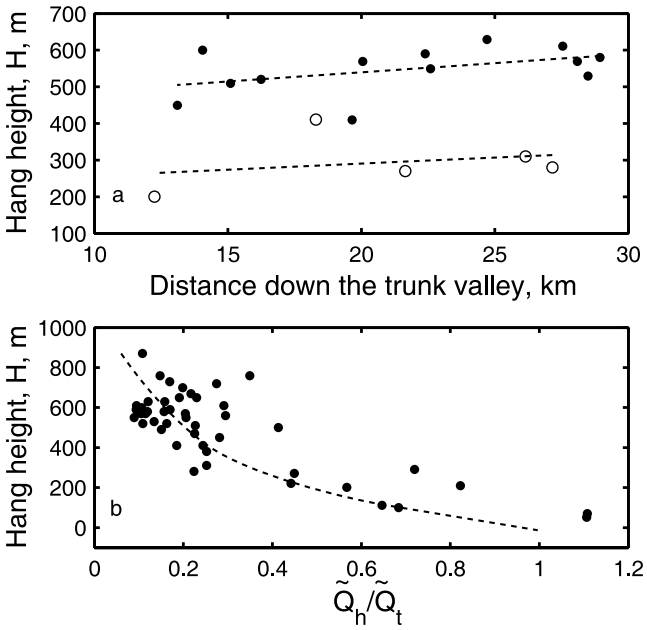

Figure 6. (a) Hang height as a function of distance down the Sunwapta trunk valley. The data are separated into two groups defined by the discharge proxy of each hanging valley, $\tilde{Q}_h$. Solid circles indicate $\tilde{Q}_h < 1000$ m, and open circles indicate 1000 m $< \tilde{Q}_h < 2000$ m. Remaining hanging valleys with values outside these ranges were not considered. (b) Hang height as a function of relative discharge proxy.

by sliding velocity, the agreement between the studies is suggestive and encouraging.

[37] The influence of velocity on bedrock erosion rate implied by our data and assumed by *MacGregor et al.* [2000] should be reconciled with knowledge of quarrying. The rate of crack growth in the bed, which is thought to limit quarrying rates, may be controlled by sliding speed through its effect on sizes of cavities downstream from bumps on the bed [e.g., *Hallet*, 1996]. In addition, sliding speed is commonly correlated to basal water pressure [*Hooke*, 2005], which likely affects the water pressure in bedrock cracks and thereby affects crack growth rates [*Iverson*, 1991]. Alternatively, quarrying rates may be limited not by rates of crack growth but by the dislodgement rate of sufficiently fractured bedrock. In some geologic settings, cracks associated with bedding planes, foliations, joints, and other planes of weakness that precede glaciation may leave little requirement for crack extension in the bed, such that the dislodgement rate of fracture-bound blocks limits the quarrying rate. Dislodgement rate may depend on sliding velocity through its effect on the bed-parallel drag on loosened rock fragments and its correlation to basal water pressure, which reduces frictional resistance to bedrock dislodgement [*Iverson*, 1991]. Our study cannot resolve these issues but highlights the need for better data regarding the mechanics of quarrying.

7. Conclusions

[38] Variability of balance velocity, as indicated by valley morphology, accounts for 60% of the total variability in hang height and for 55–85% of the hang height variability if the three catchments of the study area are considered separately. Remaining variability of hang height can be reasonably attributed to spatial variations in snow accumulation rate, glaciation duration, nonglacial erosional processes and other factors that could not be included in our analysis. Assuming that sliding velocity is a constant fraction of balance velocity, hang height variability is accounted for most fully if erosion rates are proportional to sliding velocity raised to a power of about 1/3. These results provide tentative support for velocity-based erosion rules used to model glacial erosion over large time and length scales.

Appendix A: Sliding Rule Approach

[39] Instead of simply considering sliding velocity to be a fraction of balance velocity, a sliding rule can be substituted into equation (2). Laboratory and field studies indicate that over various length scales, sliding speed, U_s, should depend on the basal shear stress, τ_b, and effective pressure, N, which is the difference between ice overburden and pore water pressure. The sliding rule is typically expressed as

$$U_s = k\frac{\tau_b^p}{N^q}, \tag{A1}$$

where k, p, and q are empirically determined constants. Values proposed for p and q range from 1 to 3 and from 0 to 2, respectively [*Paterson*, 1994, p. 153]. The precise form of this equation and the values of the "constants" are debated. For example, *Iken and Truffer* [1997] observed very different surface velocities during different years on Findelengletscher, Switzerland, although basal shear stresses and water pressures were similar. They argued that equation (A1) is incorrect, unless k is replaced with a function that depends on water pressure as well as the connectivity of the subglacial drainage system. Without knowledge of the temporal or spatial variability of water pressure, we set mean sliding velocity proportional to the basal shear stress at the glacier centerline:

$$U_s = \kappa\tau_b^p, \tag{A2}$$

where κ is a function that depends on bed roughness, water pressure, drainage system connectivity, and other factors. Inserting the relationship for basal shear stress (equation (5)) into equation (A2) gives

$$U_s = \kappa(S\rho g h \sin\alpha)^p. \tag{A3}$$

Isolating ice thickness in the continuity equation (equation (3)) and substituting the result into equation (A3) yields

$$U_s = \kappa\left(\frac{S\rho g \dot{a} A \sin\alpha}{Uw}\right)^p. \tag{A4}$$

If, as before, the sliding velocity is considered to be some fraction, λ, of the balance velocity, then

$$U_s = \left[\kappa\left(\frac{\lambda S\rho g \dot{a} A \sin\alpha}{w}\right)^p\right]^{\frac{1}{1+p}}. \tag{A5}$$

We now isolate variables in equation (A5) that both vary appreciably among glaciers in a particular region and can be estimated from the geometry of glacial valleys, and insert the result into equation (2) to obtain equations analogous to equations (6)–(8):

$$H = C_2 \Psi_2, \tag{A6}$$

where

$$C_2 = CT\kappa^{\frac{n}{1+p}}(\lambda S \rho g \dot{a})^{\frac{np}{1+p}} \tag{A7}$$

and

$$\Psi_2 = \left(\frac{A_t \sin \alpha_t}{w_t}\right)^{\frac{np}{1+p}} - \left(\frac{A_h \sin \alpha_h}{w_h}\right)^{\frac{np}{1+p}}. \tag{A8}$$

As with C_1 of equation (7), C_2 is not a constant because some of the variables in equation (A7) will differ among glaciers. However, by considering C_2 to be a constant, we test the hypothesis that its variability is small relative to Ψ_2.

[40] Like equation (6), equation (A6) is a relationship between hang height and valley morphology that can be tested with our measurements from topographic maps. Equation (A6) is the same as equation (6), except that the erosion rule exponent in equation (8), n, has been replaced with $\frac{np}{1+p}$. Our analysis with the first approach indicates that the correlation between H and Ψ_2 is optimized if $\frac{np}{1+p} = 1/3$, so $n = (2/3, 1/2, 4/9)$ for $p = (1, 2, 3)$. Thus, like the first approach, this one indicates $n < 1.0$, regardless of which of the common integer values of the sliding rule exponent, p, is chosen.

[41] **Acknowledgments.** The glaciology group at the University of Alaska Fairbanks provided constructive feedback. Comments from R. S. Anderson, B. Hallet, B. Hubbard, J. Tomkin, and S. Tulaczyk improved the manuscript.

References

Anderson, R. S., P. Molnar, and M. Kessler (2006), Features of glacial valley profiles simply explained, *J. Geophys. Res.*, *111*, F01004, doi:10.1029/2005JF000344.

Boulton, G. S. (1979), Processes of glacier erosion on different substrata, *J. Glaciol.*, *23*(89), 15–38.

Braun, J., D. Zwartz, and J. H. Tomkin (1999), A new surface-processes model combining glacial and fluvial erosion, *Ann. Glaciol.*, *28*, 282–290.

Budd, W. F., P. L. Kleage, and N. A. Blundy (1979), Empirical studies of ice sliding, *J. Glaciol.*, *23*(89), 157–170.

Clarke, G. K. C. (1991), Length, width, and slope influences on glacier surging, *J. Glaciol.*, *37*(126), 236–246.

Drewry, D. (1986), *Glacial Geologic Processes*, 374 pp., Edward Arnold, London.

Hallet, B. (1979), A theoretical model of glacial abrasion, *J. Glaciol.*, *23*(89), 39–50.

Hallet, B. (1996), Glacial quarrying: A simple theoretical model, *Ann. Glaciol.*, *22*, 1–8.

Hallet, B., L. Hunter, and J. Bogen (1996), Rates of erosion and sediment evacuation by glaciers: A review of field data and their implications, *Global Planet. Change*, *12*, 213–235.

Harbor, J. M. (1992), Numerical modeling of the development of U-shaped valleys by glacial erosion, *Geol. Soc. Am. Bull.*, *104*(10), 1364–1375.

Harbor, J. M., and D. A. Wheeler (1992), On the mathematical description of glaciated-valley cross sections, *Earth Surf. Processes Landforms*, *17*(5), 477–485.

Hooke, R. LeB. (2005), *Principles of Glacier Mechanics*, 2nd ed., 429 pp., Cambridge Univ. Press, New York.

Hughes, T. J. (1998), *Ice Sheets*, 343 pp., Oxford Univ. Press, New York.

Iken, A., and M. Truffer (1997), The relationship between subglacial water pressure and velocity of Findelengletscher, Switzerland, during its advance and retreat, *J. Glaciol.*, *43*(144), 328–338.

Iverson, N. R. (1991), Potential effects of subglacial water-pressure fluctuations on quarrying, *J. Glaciol.*, *37*(125), 27–36.

Iverson, N. R. (2002), Processes of glacial erosion, in *Glacial Environments*, edited by J. Menzies, pp. 131–146, Elsevier, New York.

Jaeger, J. B., B. Hallet, T. Pavlis, J. Sauber, D. Lawson, J. Milliman, R. Powell, S. P. Anderson, and R. S. Anderson (2001), Orogenic and glacial research in pristine southern Alaska, *Eos Trans. AGU*, *82*(19), 213–216.

Jahns, R. H. (1943), Sheet structure in granites, its origin and use as a measure of glacial erosion in New England, *J. Geol.*, *51*(2), 71–98.

Loso, M. G., R. S. Anderson, and S. P. Anderson (2004), Post-Little Ice Age record of coarse and fine clastic sedimentation in an Alaska proglacial lake, *Geology*, *32*(12), 1065–1068.

MacGregor, K. R., R. S. Anderson, S. P. Anderson, and E. D. Waddington (2000), Numerical simulations of glacial-valley longitudinal profile evolution, *Geology*, *28*(11), 1031–1034.

National Snow and Ice Data Center (2003), World Glacier Inventory, http://nsidc.org/data/g01130.html, Boulder, Colo.

Natural Resources Canada (1994a), Columbia Icefield, *Mapsheet 083C03*, scale 1:50,000, Ottawa.

Natural Resources Canada (1994b), Clemenceau Icefield, *Mapsheet 083C04*, scale 1:50,000, Ottawa.

Natural Resources Canada (1994c), Fortress Lake, *Mapsheet 083C05*, scale 1:50,000, Ottawa.

Natural Resources Canada (1994d), Sunwapta Peak, *Mapsheet 083C06*, scale 1:50,000, Ottawa.

Natural Resources Canada (1994e), Southesk Lake, *Mapsheet 083C11*, scale 1:50,000, Ottawa.

Natural Resources Canada (1994f), Athabasca Falls, *Mapsheet 083C12*, scale 1:50,000, Ottawa.

Natural Resources Canada (1994g), Medicine Lake, *Mapsheet 083C13*, scale 1:50,000, Ottawa.

Natural Resources Canada (1994h), Athabasca Pass, *Mapsheet 083D08*, scale 1:50,000, Ottawa.

Natural Resources Canada (1994i), Amethyst Lakes, *Mapsheet 083D09*, scale 1:50,000, Ottawa.

Natural Resources Canada (1994j), Jasper, *Mapsheet 083D16*, scale 1:50,000, Ottawa.

Oerlemans, J. (1984), Numerical experiments on large-scale glacial erosion, *Z. Gletscherkd. Glazialgeol.*, *20*, 107–126.

Paterson, W. S. B. (1994), *Physics of Glaciers*, 3rd ed., 480 pp., Elsevier, New York.

Riihimaki, C. A., K. R. MacGregor, R. S. Anderson, S. P. Anderson, and M. G. Loso (2005), Sediment evacuation rates and glacial erosion rates at a small alpine glacier, *J. Geophys. Res.*, *110*, F03003, doi:10.1029/2004JF000189.

Snedecor, G. W., and W. G. Cochran (1980), *Statistical Methods*, 7th ed., 507 pp., Iowa State Univ. Press, Ames.

Walder, J. S. (1986), Hydraulics of subglacial cavities, *J. Glaciol.*, *32*(112), 439–445.

Yorath, C., and B. Gadd (1995), *Of Rocks, Mountains, and Jasper—A Visitors Guide to the Geology of Jasper National Park*, 170 pp., Dundurn, Toronto, Ont., Canada.

J. M. Amundson, Geophysical Institute, University of Alaska Fairbanks, 903 Koyukuk Drive, Fairbanks, AK 99775-7320, USA. (amundson@gi.alaska.edu)

N. R. Iverson, Department of Geological and Atmospheric Sciences, Iowa State University, 253 Science I, Ames, IA 50011-3212, USA. (niverson@iastate.edu)